[2]Duranti, S., and Pittaluga, F., "Improvement of Navier–Stokes ALE Predictions by Adoption of a TSDIA Turbulence Model," *Proceedings of COST Action F1 Workshop on 3D Navier–Stokes Codes: Numerics and Modeling*, Paper 7/2, Courchevel, France, Jan. 1997.

[3]Duranti, S., Pezzuto, G., and Pittaluga, F., "Numerical Prediction of Neutral Atmospheric Boundary Layers," Symposium EACWE-2 on Wind Engineering," *Proceedings of the 2nd EACWE (European and African Conference on Wind Engineering)*, S. G. E., Padua, Italy, pp. 341–348; also *International Journal of Wind Engineering and Industrial Aerodynamics*, Vol. 74–76, Elsevier, Amsterdam, 1998, pp. 263–273.

[4]Yoshizawa, A., "Simplified Statistical Approach to Complex Turbulent Flows and Ensemble-Mean Compressible Turbulence Modeling," *Physics of Fluids*, Vol. 7, No. 12, 1995, pp. 3105–3177.

[5]Yoshizawa, A., Liou, W. W., Yokoi, N., and Shih, T. H., "Modeling of Compressible Effects on the Reynolds Stress Using a Markovianized Two-Scale Method," *Physics of Fluids*, Vol. 9, No. 10, 1997, pp. 3024–3036.

[6]Duranti, S., and Pittaluga, F., "Prediction of Complex Internal Flows by Means of a Three-Equation Turbulence Model," AIAA Paper 99-3372, July 1999.

[7]Pittaluga, F., "NAST: An Advanced 3D Compressible Navier–Stokes Solver," *Proceedings of COST Action F1 Workshop on Complex Viscous Flows*, Paper 13/2, Ecole Polytechnique Federale de Lausanne (EPFL), Lausanne, Switzerland, Oct. 1993.

[8]Amsden, A. A., Butler, T. D., and O'Rourke, P. J., "KIVA-II: A Computer Program for Chemically Reactive Flows with Sprays," Los Alamos National Lab., Rept. LA-11560-MS, Los Alamos, NM, May 1989.

[9]Le, H., and Moin, P., "Direct Numerical Simulation of Turbulent Flow over a Backward Facing Step," Center for Turbulence Research, Annual Research Briefs, Stanford Univ., Stanford, CA, 1992, pp. 161–173.

[10]Samimy, M., and Elliott, G. S., "Effects of Compressibility on the Characteristics of Free Shear Layers," *AIAA Journal*, Vol. 28, No. 3, 1990, pp. 439–445.

[11]Goebel, S. G., and Dutton, J. C., "Experimental Study of Compressible Turbulent Mixing Layers," *AIAA Journal*, Vol. 29, No. 4, 1991, pp. 538–546.

R. M. C. So
Associate Editor

Vortex Method Simulation of the Flow Around a Circular Cylinder

Angelo A. Mustto* and Gustavo C. R. Bodstein†
Federal University of Rio de Janeiro, 21945-970 Rio de Janeiro, Brazil
and
Miguel H. Hirata‡
Federal Engineering School of Itajuba, 37500-000 Itajuba, Minas Gerais, Brazil

Nomenclature

C_D, C_L	= drag and lift coefficients, respectively
k	= numerical parameter
N	= number of vortices created every time step
N_T	= total number of vortices present in the flow
P, Q	= random numbers between 0 and 1, drawn from a uniform density distribution
Re, Sr	= Reynolds and Strouhal numbers, respectively, based on the cylinder diameter
r	= radial distance from a vortex
t, Δt	= time and time step, respectively
u, v	= x and y components of velocity field
x, y	= Cartesian coordinates
z, $\bar{z}$	= complex variable, $x + iy$, and complex conjugate
Γ	= vortex strength (positive counterclockwise)
Δr, $\Delta\theta$	= radial and polar angle random increments, respectively
ε	= distance between generated vortices and cylinder surface
σ	= vortex core radius
ω	= vorticity

Subscripts

c	= convection
d	= diffusion
im	= inverse image of a vortex
θ	= circumferential direction

Introduction

THE flow around a circular cylinder is characterized by several different regimes, depending on the value of the Reynolds number. These regimes range from steady Stokes-type flows to strongly unsteady flows, where a von-Kármán-type periodic wake is formed. Among the methods reported in the literature that have been used to simulate this flow, the (Lagrangian) discrete vortex method[1–3] has been playing an important role. In this work, we propose a novel algorithm of the vortex method that is able to produce effective calculations of global quantities for flows around bluff bodies. Our objectives are 1) to develop an alternative algorithm within the Lagrangian discrete vortex method framework, where a new vorticity generation scheme is implemented; 2) to identify the influence of the numerical parameters; and 3) to calculate mean quantities of the flow and compare the results to others available in the literature.

Mathematical Background

We consider the two-dimensional, incompressible, unsteady and high-Reynolds-number flow around a circular cylinder, immersed in an unbounded region with a uniform flow upstream. This flow, started impulsively from rest, is governed by the continuity and the Navier–Stokes equations, subject to the impermeability and no-slip conditions on the cylinder, and uniform flow at infinity. Alternatively, we can use the nondimensional vorticity equation in the form

$$\frac{\partial\omega}{\partial t} + \boldsymbol{u}\cdot\nabla\omega = \frac{2}{Re}\nabla^2\omega \tag{1}$$

All of the equations are made nondimensional by the freestream speed and the cylinder radius. Because the vorticity is modeled as a cloud of discrete vortices, we can use the circle theorem[4] to construct the velocity field such that it satisfies the continuity equation, the condition at infinity, and the impermeability condition. Thus, a general expression for the complex velocity is

$$u - iv = \left(1 - \frac{1}{z^2}\right) - \frac{i}{2\pi}\sum_{n=1}^{N_T}\frac{\Gamma_n}{z - z_n(t)} + \frac{i}{2\pi}\sum_{n=1}^{N_T}\frac{\Gamma_n}{z - z_{\mathrm{im},n}(t)} \tag{2}$$

where $z_{\mathrm{im},n}(t) = 1/\bar{z}_n(t)$. From the unsteady Blasius formula,[4] the aerodynamic forces can be written as

$$C_D + iC_L = -i\sum_{n=1}^{N_T}\Gamma_n[(u_n + iv_n) - (u_{\mathrm{im},n} + iv_{\mathrm{im},n})] \tag{3}$$

Numerical Method and Implementation

The numerical method is implemented in five steps: 1) vorticity generation, 2) calculation of the forces on the body, 3) convection of the vortices, 4) diffusion of the vortices, 5) elimination of some vortices, and 6) stepping in time. The vorticity generation is carried out as follows. At each time step, N new vortices are created a small distance ε off the body surface, at a radial distance $1 + \varepsilon$, with a uniform angular distribution. Their strengths are determined by imposing the no-slip condition at $N - 1$ points on the cylinder

Presented as Paper 98-2409 at the AIAA 16th Applied Aerodynamics Conference, Albuquerque, NM, 15–18 June 1998; received 5 February 1999; revision received 3 November 1999; accepted for publication 16 December 1999.

*Graduate Student, Department of Mechanical Engineering, EE/COPPE, C.P. 68503.

†Associate Professor, Department of Mechanical Engineering, EE/COPPE, C.P. 68503. Senior Member AIAA.

‡Visiting Professor, Department of Mechanics, IEM, C.P. 50.

surface, right underneath the newly created vortices. The velocities due to the freestream flow, the dipole, and all of the vortices in the wake (and their images) are computed at the $N-1$ points of the cylinder surface, and this contribution is added to the velocities induced by the new vortices (and their images) and equated to zero. Thus, $N-1$ equations can be written out for the N unknowns (the strengths of the new vortices). The Nth equation is a statement of conservation of circulation, where the sum of all vortices, with known and unknown strengths, must equal zero. This procedure yields an algebraic system of N equations and N unknowns. The elements of the $N \times N$ matrix depend only on the positions of the vortices just created and on the points on the cylinder surface where the no-slip condition is imposed and are calculated only once for the simulation. The right-hand side of the system is recalculated every time step. Vortices that penetrate the body are eliminated, and the lost circulation is compensated for in the next time step.

Vorticity convection and diffusion are simulated using the operator-splitting algorithm,[1] that is,

$$\frac{\partial \omega}{\partial t} + \boldsymbol{u} \cdot \nabla \omega = 0 \tag{4a}$$

$$\frac{\partial \omega}{\partial t} = \frac{2}{Re} \nabla^2 \omega \tag{4b}$$

For the convective process, governed by Eq. (4a), the Lagrangian motion of each vortex is determined by integration of the vortex path equation. Using a first-order Euler scheme, we have

$$\Delta \boldsymbol{x}_c = \boldsymbol{u} \Delta t \tag{5}$$

where $\boldsymbol{u}$ is calculated from Eq. (2). The process of viscous diffusion, governed by Eq. (4b), is simulated using the random walk method,[5] where the vortex displacements are

$$\Delta x_d = \Delta r \cos(\Delta \theta) \tag{6a}$$

$$\Delta y_d = \Delta r \sin(\Delta \theta) \tag{6b}$$

$$\Delta r = [\, 8Re^{-1} \Delta t \ell n(1/P)]^{\frac{1}{2}} \tag{7a}$$

$$\Delta \theta = 2\pi Q \tag{7b}$$

To desingularize the point vortices, we use Lamb vortices for $r \leq \sigma$, whose velocity is

$$u_\theta = (\Gamma / 2\pi r)\{1 - \exp[-5.0257(r^2/\sigma^2)]\} \tag{8}$$

The core radius, kept constant during the simulation, is given by $\sigma = 6.3408(\Delta t/Re)^{1/2}$, which provides a difference between the induced velocity of a point vortex and Eq. (8) of less than 0.6%. Based on a convective length scale of order $2\pi/N$ (characterizing the distance between adjacent vortices generated at the surface) and a velocity scale of the order of the freestream speed, the time step is estimated from $\Delta t = 2\pi k/N$. The parameter k, where $0 < k < 1$, represents an upper bound on the maximum allowed convective step of a vortex; in the computations we used $k = 0.25$. These equations for σ and Δt provide nominal values for these parameters. We also set the distance ε off the cylinder surface equal to σ for all of the cases studied.

Results and Discussion

The results presented hereafter refer to $Re = 1.0 \times 10^5$. For this (high) value, the boundary layer is still laminar prior to separation, although the wake is turbulent. According to the experimental results of Blevins,[6] $C_D = 1.20$ and $Sr = 0.19$, with 10% uncertainty. The results of the simulations for all the cases studied, obtained for a long dimensionless time ($t \geq 45$), are shown in Table 1. Cases 1 and 9 use nominal values of the numerical parameters, and the other cases allow for a sensitivity analysis of these parameters to be carried out. As the value of ε increases with respect to case 1 (e.g., case 2), for $N = 16$ and fixed Δt, the value of C_D increases and that of the Strouhal number decreases, approaching the experimental ones. When ε goes from 0.0032 to 0.0128 (cases 3–7) there is again a monotonic increase of C_D and a monotonic decrease of Strouhal number. The same trends are observed with respect to case 9 (e.g., case 8), for $N = 32$ and fixed Δt. Comparison of cases 1 and 5 (for $N = 16$), or cases 9 and 11 (for $N = 32$), keeping ε constant, shows that reducing Δt yields better estimates of C_D and Strouhal number. For $N = 32$, case 9 provides more accurate results than case 1, and, therefore, the equations for σ (and ε) and Δt provide better estimates of these parameters. The effect of increasing N, keeping Δt and ε fixed, can also be seen when we compare case 8 with case 3, case 9 with case 4, and case 10 with case 6. For these comparisons, an increase in N also increases the value of C_D and decreases Strouhal number. Higher values of N causes the computation to become more expensive because the operation count of the algorithm is proportional to N_T^2. A fast-summation scheme, such as the multipole technique,[7] corrects this problem.

Table 1 Numerical parameters, $Re = 1.0 \times 10^5$

Case	N	Δt	$\sigma = \varepsilon$	C_D	Sr
1[a]	**16**	**0.10**	**0.0064**	**0.79**	**0.25**
2	16	0.10	0.0128	1.16	0.22
3	16	0.05	0.0032	0.88	0.28
4	16	0.05	0.0045	1.05	0.26
5	16	0.05	0.0064	1.23	0.23
6	16	0.05	0.0080	1.36	0.22
7	16	0.05	0.0128	1.41	0.21
8	32	0.05	0.0032	1.13	0.24
9	**32**	**0.05**	**0.0045**	**1.22**	**0.22**
10	32	0.05	0.0080	1.42	0.20
11	32	0.10	0.0045	0.84	0.25
12	32	0.10	0.0064	1.06	0.23

[a]Boldface indicates nominal parameters.

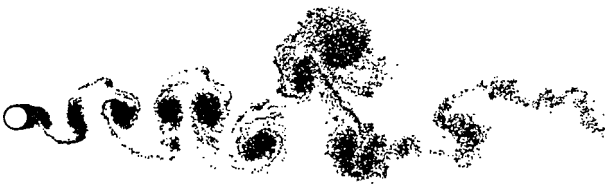

Fig. 1 Position of the wake vortices at $t = 60$ for case 9.

The properties of the numerical method can be described as follows. The equation for Δt provides a stability criterion through the choice of k and N, where N is chosen as large as possible. Because the velocity is a random variable, the convergence of the method can be expected only in the mean,[1] and it can be appreciated as Δt decreases or N increases because the Strouhal number approaches the experimental value 0.19. For this flow the Strouhal number is relatively insensitive to the three-dimensional[8] and turbulence effects present in the experiments, as opposed to C_D, which is expected to be higher in the simulations than in the experiments. From the accuracy viewpoint, the random walk method produces errors proportional to $\sqrt{(\Delta t/Re)}$, whereas the error due to the convection algorithm is proportional to Δt. N must be as large as possible to maintain a minimum number of new vortices in the flow, given that each vortex has an increasing number of opportunities to cross the cylinder surface and disappear as Δt is reduced. Finally, Table 1 clearly shows that the results improve their accuracy as ε increases, for fixed Δt and N. This trend has not been reported in the literature so far.

Figure 1 shows the position of the wake vortices for case 9 at $t = 60$. We can clearly observe the separation and the vortex formation, shedding, and pairing processes. The variation in time of the aerodynamic forces (Fig. 2) shows that, as soon as the steady periodic regime is reached, the lift coefficient oscillates about zero with a Strouhal number about twice the frequency of the drag coefficient. Comparing case 9 with the experimental results, we note a 1.7% difference in C_D and 15.8% difference in Strouhal number.

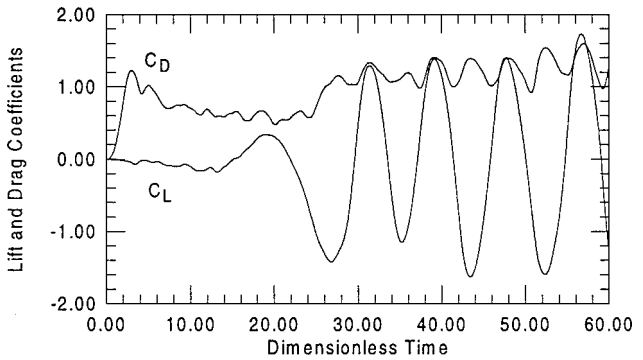

Fig. 2 Variation of C_D and C_L with time for case 9.

Ogami and Ayano[2] computed $C_D = 1.07$, using a Lagrangian viscous vortex method (they did not calculate the Strouhal number). The general agreement between the two numerical methods is acceptable for the mean drag coefficient, and both results are close to the experimental values. However, the three-dimensional and turbulence effects present in the experiments are nonnegligible for the Reynolds number used in the simulations, and a two-dimensional computation must produce higher values for the drag coefficient, as obtained in our simulation.

Conclusions

The vortex method presented here to study the two-dimensional, incompressible, unsteady flow around a fixed circular cylinder is able to predict the main global quantities of a high-Reynolds-number flow. The calculated aerodynamic forces are close to the experimental and numerical data used for comparison. Also, the simulations are able to capture complex flow mechanisms, such as separation, as part of the computation. The analysis of the influence of the numerical parameters on the simulation has pointed out the importance of choosing suitable values for N, Δt, and ε, and the trends when these parameters are varied have also been identified. The numerical results also brought up that ε strongly affects the simulations and, therefore, must be modeled correctly. This is an important output of this work.

Acknowledgments

The authors acknowledge the Conselho Nacional de Desenvolvimento Científico e Tecnológico (National Council for Scientific and Technological Development), under Grants 521260/94-9 and 143041/97-5, and the Fundação de Amparo à Pesquisa do Estado de Minas Gerais (Foundation for Research Support of the State of Minas Gerais), under Grant TEC-1565/97, for the financial support of this project.

References

[1]Chorin, A. J., "Numerical Study of Slightly Viscous Flow," *Journal of Fluid Mechanics*, Vol. 57, Pt. 4, 1973, pp. 785–796.

[2]Ogami, Y., and Ayano, Y., "Flows Around a Circular Cylinder Simulated by the Viscous Vortex Model—The Diffusion Velocity Method," *Computational Fluid Dynamics Journal*, Vol. 4, No. 3, 1995, pp. 383–399.

[3]Sarpkaya, T., "Vortex Element Methods for Flow Simulation," *Advances in Applied Mechanics*, Vol. 31, 1994, pp. 113–247.

[4]Milne-Thomson, L. M., *Theoretical Hydrodynamics*, Macmillan, London, 1968, pp. 157, 158, 255, 256.

[5]Lewis, R. I., *Vortex Element Methods for Fluid Dynamic Analysis of Engineering Systems*, Cambridge Univ. Press, Cambridge, England, U.K., 1991, pp. 372–374.

[6]Blevins, R. D., *Applied Fluid Dynamics Handbook*, Van Nostrand Reinhold, New York, 1984, pp. 313–317.

[7]Greengard, L., and Rokhlin, V., "A Fast Algorithm for Particle Simulations," *Journal of Computational Physics*, Vol. 73, No. 2, 1987, pp. 325–348.

[8]Prasad, A., and Williamson, C. H. K., "Three-Dimensional Effects in Turbulent Bluff-Body Wakes," *Journal of Fluid Mechanics*, Vol. 343, July 1997, pp. 235–265.

J. Kallinderis
Associate Editor

Vibration Analysis of Thick Laminated Composite Cylindrical Shells

K. Y. Lam,* T. Y. Ng,† and Wu Qian‡
National University of Singapore, Singapore 118261, Republic of Singapore

Introduction

THE development of thin-plate and shell theories has received much attention over the past century,[1–3] but only more recently has attention been drawn to thick-plate and shell theories with consideration of transverse shear deformation in multilayered composite plates and shells. Reddy[4] developed a simple higher-order theory for laminated composite plates where the two transverse shear stresses vanish on the top and bottom surfaces and the displacement field is formed by setting the two corresponding strains to zero. Soldatos and Hadjigeorgiou[5] employed the governing equations of three-dimensional linear elasticity and solved them by using an iterative approach for the prediction of the frequencies of vibration.

Voyiadjis and Shi[6] developed a refined higher-order, two-dimensional theory for thick cylindrical shells with very good approximations for the shell constitutive equations and the nonlinear distributions of in-plane stresses across the thickness of the shell. On the basis of shear deformation theory, Kabir and Chaudhuri[7] used a double Fourier series to obtain analytical solution of the free vibration of antisymmetrical angle-ply laminated shells. Soldatos[8] developed a refined shear deformable theory that accounts for parabolic variation of transverse shear strains and is capable of satisfying zero shear traction boundary conditions at the external shell or plate surface without making use of transverse shear correction factors. An approach based on Galerkin's method was used to solve the problem. Touratier[9] provided a generalized shear deformation theory for axisymmetrical multilayered shells. The shear forces were taken into account using "shear" functions introduced in the assumed kinematics. In the vibration and stability analyses of cross-ply laminated cylindrical shells, Nosier and Reddy[10] developed a new technique by generating Levy-type solutions and using an extension of Donnell's classical equations to first-order shear deformation theory.

In this Note, an improved general higher-order, thick-laminated-shell theory is established to analyze vibration of thick cylindrical shells. There are five unknowns in this theory, as in the first-order theory, but they have different physical meanings and include two additional rotations due to transverse shear forces. The theory is based on a summation of displacements of classic thin-shell theory and displacements due to transverse shear forces. The displacements due to transverse shear forces are in the form of cubic functions of the thickness coordinate that satisfy the parabolic distribution of the transverse shear stresses and zero transverse normal strain. The minimum total potential energy principle is used to obtain the frequencies of cylindrical shells. The effect of transverse shear force resultants on frequency characteristics has been studied by investigating the frequency variations with transverse shear correction factor K. Numerical results of the higher-order shear deformation theory and the first-order shear deformation theory are compared with existing results in the literature. The frequency characteristics for thick laminated composite cylindrical shells with different thickness-to-radius H/R and length-to-radius L/R ratios is presented

Received 26 April 1999; revision received 8 July 1999; accepted for publication 9 July 1999.

*Director and CEO, Institute of High Performance Computing, 89B Science Park Drive, 01-05/08, The Rutherford, Singapore Science Park 1.

†Principal Research Engineer, Institute of High Performance Computing, 89B Science Park Drive, 01-05/08, The Rutherford, Singapore Science Park 1.

‡Research Engineer, Institute of High Performance Computing, 89B Science Park Drive, 01-05/08, The Rutherford, Singapore Science Park 1.